5120–5132 *Nucleic Acids Research, 2005, Vol. 33, No. 16*
doi:10.1093/nar/gki828

RNase P: role of distinct protein cofactors in tRNA substrate recognition and RNA-based catalysis

Ela Sharin, Aleks Schein, Hagit Mann, Yitzhak Ben-Asouli and Nayef Jarrous*

Department of Molecular Biology, The Hebrew University-Hadassah Medical School, Jerusalem 91120, Israel

Received January 24, 2005; Revised May 22, 2005; Accepted August 24, 2005

ABSTRACT

The *Escherichia coli* ribonuclease P (RNase P) has a protein component, termed C5, which acts as a cofactor for the catalytic M1 RNA subunit that processes the 5′ leader sequence of precursor tRNA. Rpp29, a conserved protein subunit of human RNase P, can substitute for C5 protein in reconstitution assays of M1 RNA activity. To better understand the role of the former protein, we compare the mode of action of Rpp29 to that of the C5 protein in activation of M1 RNA. Enzyme kinetic analyses reveal that complexes of M1 RNA–Rpp29 and M1 RNA–C5 exhibit comparable binding affinities to precursor tRNA but different catalytic efficiencies. High concentrations of substrate impede the activity of the former complex. Rpp29 itself exhibits high affinity in substrate binding, which seems to reduce the catalytic efficiency of the reconstituted ribonucleoprotein. Rpp29 has a conserved C-terminal domain with an Sm-like fold that mediates interaction with M1 RNA and precursor tRNA and can activate M1 RNA. The results suggest that distinct protein folds in two unrelated protein cofactors can facilitate transition from RNA- to ribonucleoprotein-based catalysis by RNase P.

INTRODUCTION

Biosynthesis of cellular RNA, e.g. mRNA, rRNA and tRNA, requires small nuclear and nucleolar ribonucleoproteins, some of which have a large number of protein subunits (1–4). While main efforts are being made in elucidating the roles of the RNA moieties of these catalytic ribonucleoproteins in biological processes (5–7), the precise functions of their protein components remain largely unknown. One of these catalytic ribonucleoproteins is ribonuclease P (RNase P), a ubiquitous tRNA processing endonuclease (8–10). Highly purified human nuclear RNase P has a single species of RNA, H1 RNA, which is associated with at least 10 distinct protein subunits, Rpp14, Rpp20, Rpp21, Rpp25, Rpp29, Rpp30, Rpp38, Rpp40, hPop1 and hPop5 (11–16). Reconstitution of the endonucleolytic activity of human RNase P reveals that H1 RNA and two conserved protein subunits, Rpp21 and Rpp29 (13,14), are sufficient for the removal of 5′ leader sequence from precursor tRNA *in vitro* (17). This finding raised the concept that binding and cleavage of precursor tRNA substrates by eukaryotic RNase P may need a few protein components. Reconstitution systems developed for active archaeal RNase P ribonucleoproteins support this concept (18,19).

The role of the subunit Rpp29 in RNA-based catalysis is highlighted by the ability of this protein to activate the M1 RNA enzyme of *Escherichia coli* RNase P at low concentrations of magnesium ions (17). Archaeal/eukaryal Rpp29 proteins are central components in the assembly and function of RNase P (19–22). Archaeal Rpp29 polypeptides are smaller in size, when compared with their eukaryal counterparts and have structural features found in bacterial and eukaryal proteins, as revealed from the determination of their NMR and crystal structures (19,22–24). A prominent structural feature of *Archaeoglobus fulgidus* Rpp29 is a sheet of six antiparallel β-strands wrapped around a core of conserved hydrophobic amino acids (19). The *Methanothermobacter thermoautotrophicus* Rpp29 has a β-barrel core and unstructured N- and C-terminal domains containing highly conserved amino acid residues (19). The crystal structures of *Pyrococcus horikoshii* Rpp29 (Ph1771p) and *A.fulgidus* Rpp29 reveal that their β-barrel cores are similar to those of Sm proteins and their N- and C-termini form flexible helical structures (22,24). These two archaeal Rpp29 proteins, which are structurally related to the bacterial transcription factors Hfq and NusG, as well as to the eukaryal Sm RNA-binding proteins, show similarity to the C-terminal domain of human Rpp29 (22,24).

The comparison of the mode of action of Rpp29 to that of the C5 protein in activation of M1 RNA (17,25) may provide

*To whom correspondence should be addressed. Tel: +972 2 6758233; Fax: +972 2 6784010; Email: jarrous@md.huji.ac.il

The authors wish it to be known that, in their opinion, the first two authors should be regarded as joint First Authors

new insights into the role of these cofactors in tRNA substrate recognition and RNA-based catalysis. The C5 protein has been shown to enhance the catalytic efficiency of M1 RNA and increase substrate versatility (26). Cysteine-substituted mutants of C5 proteins and *Bacillus subtilis* RNase P proteins associated with their corresponding RNA subunits can be crosslinked to the 5′ leader sequence of precursor tRNA (27–29). These A- and B-type of bacterial RNase P proteins augment the magnesium ion affinity of enzyme-substrate intermediates by correctly positioning the substrate (29). The bacterial RNase P protein stabilizes the holoenzyme against electrostatic repulsion and increases the turnover rate (30), possibly by favoring contact of the holoenzyme with the substrate over the product (31,32).

The identity among the amino acid sequences of the A- and B-type proteins of bacterial RNase P is notably low (33,34), but they share a short stretch of basic sequence, the RNR motif, a central cleft and a few aromatic amino acid residues close to their N-termini (35). Nonetheless, both types of proteins can activate the other type of bacterial RNase P RNA (24,36), as well as archaeal RNase P RNA (37). Thus, common structural features and biochemical properties of these protein cofactors facilitate RNA-based catalysis (35). However, the C5 protein and Rpp29 do not share an apparent identity at their primary amino acid sequences and thus the molecular basis for the observed activation of M1 RNA by these two cofactors (17) is unclear.

We here address some properties of Rpp29 in activating M1 RNA and compare them to those of the C5 protein known to function in substrate recognition and catalysis. The results support the idea that activation of M1 RNA by these two evolutionarily unrelated protein cofactors is based on the use of distinct protein folds that perform parallel functions.

MATERIALS AND METHODS

Site-directed mutagenesis of Rpp29

QuickChange® site-directed mutagenesis kit (Stratagene, CA) was utilized to introduce substitutions of amino acids in Rpp29 using designed primers and pHTT7K/Rpp29 as template for PCR (17), following the manufacturer's instructions. Mutations were verified by DNA sequencing.

For construction of Rpp29Δ1-124, two primers, one encompassing the codon that corresponds to methionine at position 125 and downstream sequences of Rpp29, and the other covering the translation stop codon and upstream sequences, were utilized for PCR using Rpp29 cDNA as a template. The PCR product was digested with NdeI and BamHI (sites located in the primers) and subcloned in-frame with the six histidine residues of pHTT7K, which was digested with Nde I and BamHI.

Preparation of recombinant Rpp29 proteins

Wild-type and mutant Rpp29 polypeptides were purified subsequent to their overexpression for 4 h in an *E.coli* strain BL21 (1). Fractionation of cell extracts revealed that these polypeptides were present in the P30 pellet obtained after centrifugation at 30 000× *g*. These proteins aggregate and form inclusion bodies that required to be solubilized in 1× binding buffer containing 6 M urea before loading onto nickel-charged His-Bind resin chromatography columns (Novagen). This step was followed by extensive wash of the column with 50 bed volumes of 1× binding buffer, containing 30–60 mM imidazole. Bound proteins were eluted with a gradient of 30–500 mM imidazole. Proteins were assayed for activation of M1 RNA and split into small aliquots and stored at −80°C.

Purified Rpp29 proteins were placed in 1 ml dialysis tubes (GeBAflex-tube, 3.5K; Gene Bio-Application, Israel) and subjected to sequential dialysis in 2 l volume of DA buffers (50 mM Tris–HCl, pH 8.0, 50 mM NaCl, 0.05% IGEPAL and 1 mM $MgCl_2$) that contained 4 M urea, 2 M urea and then without urea. This step was followed by ultracentrifugation of the protein at 100 000× *g* in a Beckman TLA-55 rotor at 4°C for 2 h. Protein aggregation was observed at the bottom of the tube and therefore aliquots of Rpp29 from the upper phase were collected and stored at −80°C. For gel filtration column (see below) the Rpp29 protein was sequentially dialyzed as described above but in 1× PA150 buffer (50 mM Tris–HCl, pH 7.5, 0.1 M NH_4Cl, 1 mM $MgCl_2$ and 150 mM NaCl).

Preparation of RNA and determination of 5′ end group of tRNA

A plasmid that harbors the *Schizosaccharomyces pombe* precursor $tRNA^{Ser}$ (CUA), p*SupS1*, which lacks 3′ CCA sequence, was linearized by *Taq* I and transcription was done with SP6 RNA polymerase (Promega) in the presence of 80 μCi of [α-^{32}P]UTP. After DNase I treatment, Urea Dye (xylene cyanol 0.005%; bromphenol blue 0.005% and 9 M urea) and 1–2 μl of phenol were added. The reaction products were separated in 8% polyacrylamide gel/7 M urea and the 110 nt labeled p*SupS1* was excised from the gel, extracted and ethanol precipitated. Radioactivity (in counts per minute) was determined by Bioscan QC 2000 beta-counter. The specific activity of p*SupS1* was $\sim 3 \times 10^6$ c.p.m. per 1 μg of RNA.

For preparation of mature tRNA, ^{32}P-labeled p*SupS1* or *E.coli* precursor $tRNA^{Tyr}$Su3, was first processed by M1 RNA and then the tRNA product was gel purified.

The plasmid pJA2 carrying the gene encoding M1 RNA was linearized by Fok I and RNA was transcribed *in vitro* by using T7 RNA polymerase in 100 μl total volume for 5 h. After DNA digestion with 1 U of DNase I, RNA was passed twice through G-50 spin columns prewashed with 1× TS buffer (10 mM Tris–HCl, pH 7.8, and 100 mM NaCl). For labeling of M1 RNA, 80 μCi of [α-^{32}P]UTP was added to the transcription reaction and the 377 nt M1 RNA was gel extracted as described above for precursor tRNA.

Determination of 5′ end group of tRNA, generated from processing of [α-^{32}P]ATP-labeled p*SupS1* by 2D thin layer chromatography has been described previously (17).

Reconstitution assays of M1 RNA with Rpp29

M1 RNA was incubated with wild-type or mutant Rpp29 protein in 39 μl of 1× RP buffer (17), which is a mixture of 1× MRP buffer (20 mM Tris–HCl, pH 7.5, 10 mM $MgCl_2$, 40 mM KCl, 20 μg/ml BSA, 0.2 U of rRNasin, 1 mM DTT and 1 μg of poly I:C RNA) and 1× TNET buffer (20 mM Tris–HCl, pH 7.5, 35 mM NaCl, 0.1 mM

Na_2EDTA [disodium salt], 0.01% Triton X-100 and 1 mM β-mercaptoethanol), each added separately to the reaction. After preincubation for 5–10 min on ice, labeled precursor tRNA was added and the cleavage reaction proceeded for the indicated time points at 37°C. Cleavage products were separated in 8% polyacrylamide/7 M urea gel or 12% sequencing gel. Bands were visualized by autoradiography and quantified by using Scion Image software.

Determination of kinetic parameters

For the determination of V_{max} and K_m, M1 RNA was incubated in 1× RP buffer with recombinant C5 protein, Rpp29 or mutant Rpp29 in molar concentrations indicated in each experiment. After 5 min incubation on ice, various substrate concentrations, made of mixtures of unlabeled precursor tRNA and 0.07 pmol labeled precursor tRNA, were added to the reconstituted complexes for 5–10 min on ice in 100–150 µl total volumes. Cleavage reactions proceeded at 37°C for the indicated time points, at which small aliquots of 10 µl each were withdrawn and mixed immediately with 10 µl of Urea dye. Cleavage products were separated in denaturing 8% polyacrylamide gels and substrate and products were quantified by using Scion Image software. Michaelis–Menten and Lineweaver–Burk plots and calculated parameters were according to Sigma Plots and GraphPad Prizm 4 software (17).

Electrophoretic mobility shift analysis

A ^{32}P-labeled precursor tRNA (10 000 c.p.m.; 0.07 pmol) and excess amount (0.5–1 µg) of poly(I:C) RNA were incubated in 100 µl total volumes with wild-type or mutant Rpp29 protein in 2× TNET buffer for 30 min on ice. In some experiments incubation was in 1× MK buffer (10 mM Tris–HCl, pH 7.5, 150 mM KCl, 2 mM $MgCl_2$ and 5% glycerol) for 15 min on ice and then for 10 min at room temperature. In binding assays with labeled M1 RNA, 500–1000 c.p.m. of internally labeled M1 RNA transcript was used in 100 µl total volumes. Protein–RNA complexes were separated in native 4% polyacrylamide gels (40:0.5 of acrylamide/bis). Because of the low resolution capacity of native gels, complexes obtained in the presence of mature tRNA or precursor tRNA were retarded to close positions. Bands were visualized by autoradiography and quantified.

Northwestern blot analysis

Equal amounts (20 pmol) of purified proteins were separated in 12% SDS–PAGE, transferred to nitrocellulose membrane (Schleicher & Schuell) and stained with Ponceau red dye (Sigma). The membrane was washed in 2× TNET buffer containing 100–200 mM NaCl and 0.2% BSA for 1 h, and then hybridized with 1×10^6 c.p.m. of ^{32}P-labeled precursor tRNA, M1 RNA or RNase MRP RNA in 2× TNET buffer without BSA. After 1 h incubation at room temperature with constant shaking, the membrane was washed three times in 2× TNET buffers that contained 100–200 mM NaCl, rinsed briefly with water and exposed to X-ray film. As described in some experiments, the membrane was first blocked with an excess amount (5 µg) of unlabeled M1 RNA or precursor tRNA before proceeding to the hybridization step.

Oligonucleotide binding interference assays

Antisense deoxyoligonucleotides were allowed to anneal to labeled p*SupS1* (0.07 pmol) in 1× BB buffer (10 mM Tris–HCl, pH 7.5, 150 mM KCl, 1 mM DTT, 2 mM $MgCl_2$ and 5% glycerol) containing 1–3 µg of poly(I:C) RNA. After annealing for 10 min on ice, 20 pmol of Rpp29 were added for a 40 µl final volume and binding was performed for 10 min on ice and 10 min at room temperature. Complexes were resolved in non-denaturing 4% polyacrylamide gel. Substrate and products were quantified by using Scion Image software.

UV-crosslinking of Rpp29 to precursor tRNA

A ^{32}P-labeled p*SupS1* or its mature tRNA form (without 5′ leader sequence) was incubated with recombinant Rpp29 protein in 1× TNET buffer containing 2 mM $MgCl_2$ for 30 min on ice. Samples (in total volume of 100 µl) were left untreated or subjected to UV irradiation (UV light at 254 nm) for 90 s using Hoefer UVC500 crosslinker. An excess amount (up to 1000-fold) of cold p*SupS1* or mature tRNA transcripts was then added as specified. After 10 min at room temperature, samples were resolved in native 4% polyacrylamide gel and bands were visualized by autoradiography.

RESULTS

Wild-type and mutant Rpp29 proteins alter the cleavage specificity of M1 RNA

M1 RNA cleaves the *S.pombe* precursor $tRNA^{Ser}$ (CUA), p*SupS1*, between positions A27 and G28 (17). This mis-cleavage by M1 RNA can be corrected in the presence of its protein cofactor C5, so that the reconstituted holoenzyme cleaves between positions G28 and G29 (17). We examined if the cleavage specificity of M1 RNA can be corrected by recombinant Rpp29 and two deletion mutants, Rpp29Δ194-220 and Rpp29Δ162-220, which lack the last 27 and 59 amino acid residues, respectively (17). The four protein cofactors tested in the presence of M1 RNA were all able to adjust cleavage at position G28, thus releasing larger 5′ leader sequences from p*SupS1* (Figure 1A, arrows). This 1 nt change in the cleavage position has been confirmed by analysis of cleavage products of p*SupS1* in an 8% sequencing gel (Figure 1B). M1 RNA alone was inactive at 10 mM $MgCl_2$ (Figure 1B, lane 3).

The 2D thin layer chromatography revealed pGp as the 5′ end group of tRNA products generated in cleavage reactions of p*SupS1* by M1 RNA (Figure 1C, left panel) or M1 RNA-Rpp29 (Figure 1C, right panel).

The results described above demonstrate that Rpp29 directs M1 RNA to accurately recognize its substrate and hydrolyze the phosphodiester bond.

Some kinetic parameters of substrate cleavage by M1 RNA reconstituted by various protein cofactors

We determined the time course of cleavage of 0.07 µM of p*SupS1* by 0.025 µM of M1 RNA reconstituted with 0.25 µM of C5 protein or with 0.25 µM of wild-type or mutant Rpp29 proteins (Figure 2). M1 RNA–C5 cleaved ∼50% of the substrate within 16 min (Figure 2A and C), while M1 RNA–Rpp29 processed <30% of the substrate after ∼1 h of

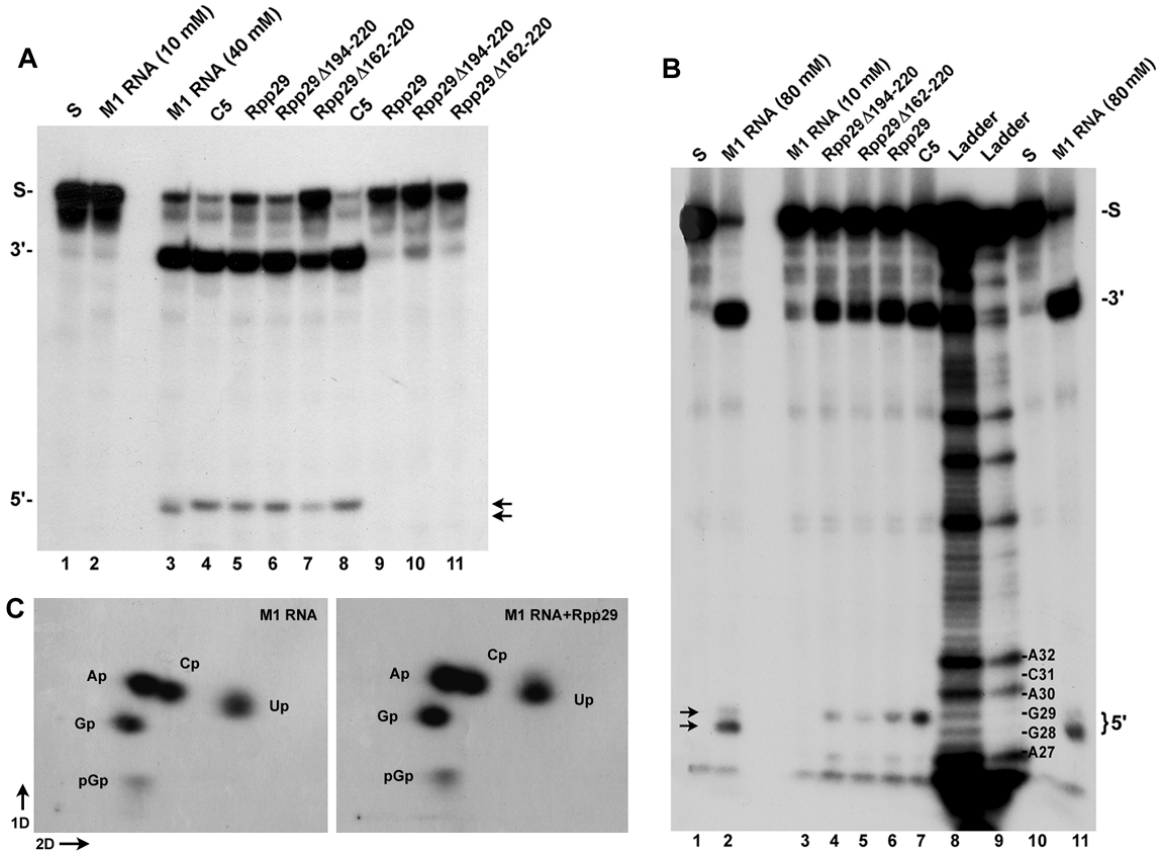

Figure 1. Cleavage specificity of M1 RNA reconstituted by various protein cofactors. (**A**) M1 RNA (0.7 pmol) was tested for processing of p*SupS1* (S) in 1× RP buffer (pH 7.5) containing 10 mM $MgCl_2$ in the absence (lane 2) or presence of 7 pmol of C5 protein (lanes 4 and 8) or 7 pmol of wild-type Rpp29 (lane 5), Rpp29Δ194-220 (lane 6) or Rpp29Δ162-220 (lane 7) (Materials and Methods). The cleavage reactions proceeded for 2 h at 37°C. As positive control, M1 RNA alone was tested in 1× RP buffer containing 40 mM $MgCl_2$ (lane 3). The recombinant proteins alone show no activity (lanes 9–11). The cleavage products, tRNA (3′) and 5′ leader sequence (5′), were resolved in 8% polyacrylamide/7 M urea gel. Arrows point to the cleavage sites at positions A27 and G28 (17). (**B**) Processing of p*SupS1* by M1 RNA alone (lanes 3) or by M1 RNA reconstituted with Rpp29Δ194-220 (lane 4), Rpp29Δ162-220 (lane 5), Rpp29 (lane 6) or C5 protein (lane 7). The conditions of the cleavage reactions were as described in (A) but the cleavage products were separated in an 8% sequencing gel. M1 RNA activated by 80 mM $MgCl_2$ primarily cleaved at position A27 (lanes 2 and 11), while M1 RNA reconstituted with the various protein cofactors cleaved at position G28. RNA ladders were obtained by partial digestion of p*SupS1* by RNase T2 (lanes 8 and 9). Arrows point to the two cleavage sites at A27 and G28. Some RNA degradation (lane 1) is seen in the gel front. (**C**) The 2D thin layer chromatography of tRNA products of cleavage reactions of p*SupS1* by M1 RNA (left panel) and M1 RNA–Rpp29 (right panel). Gp, Ap, Cp, Up and pGp are shown. Arrows point to the first and second dimension of the chromatography.

incubation (Figure 2B and C). M1 RNA reconstituted by Rpp29Δ194-220 or Rpp29Δ162-220 was less effective than M1 RNA–Rpp29 in processing of p*SupS1* (Figure 2A–C).

Based on the above results, additional multiple turnover reactions were carried in the presence of a range of p*SupS1* concentration and Lineweaver–Burk plots were prepared for M1 RNA–C5 (Figure 2D), M1 RNA–Rpp29 (Figure 2E) and M1 RNA–Rpp29Δ194-220 (Figure 2F) (Materials and Methods). In the case of M1 RNA–C5 and M1 RNA–Rpp29, the dependence of the reaction rates on substrate concentrations exhibited saturation kinetics, and therefore the results were fit to Michaelis–Menten equation, producing values for the kinetic parameters k_{cat}, K_m and k_{cat}/K_m (Table 1).

M1 RNA–C5 had a K_m value of 0.2 μM, which was ∼2-fold lower than the K_m value obtained for M1 RNA–Rpp29 or M1 RNA–Rpp29Δ194-220 (Table 1). Similar K_m values were reported for other prokaryotic precursor tRNAs cleaved by M1 RNA–C5 and under different reconstitution conditions (25). The turnover rate, k_{cat}, obtained for M1 RNA–Rpp29 was 5.2 min^{-1}, while the k_{cat} for M1 RNA–C5 was 18 min^{-1} (Table 1). Based on k_{cat} and k_{cat}/K_m values, Rpp29 was less effective by several folds than the C5 protein in activation of M1 RNA (Table 1). Nonetheless, the turnover rate and catalytic efficiency calculated for M1 RNA–Rpp29 imply that this complex is a genuine catalytic ribonucleoprotein.

Rpp29Δ194-220 was less effective than Rpp29 in activation of M1 RNA with a k_{cat} value of 3.4 min^{-1} (Table 1). Rpp29Δ162-220 was defective in activation of M1 RNA and the calculated V_{max} of the cleavage reaction was notably low (Table 1). Therefore, valid K_m or k_{cat} values could not be obtained for this latter mutant protein (Table 1). These kinetic parameters suggest that the region spanning amino acids 162–194 in Rpp29 is critical for its function as a protein cofactor (see below).

We performed additional reconstitution assays but this time in the presence of substrate concentrations that were above and below the K_m values obtained as above. Thus, time course assays were perform with 0.05–1 μM of p*SupS1*, while the

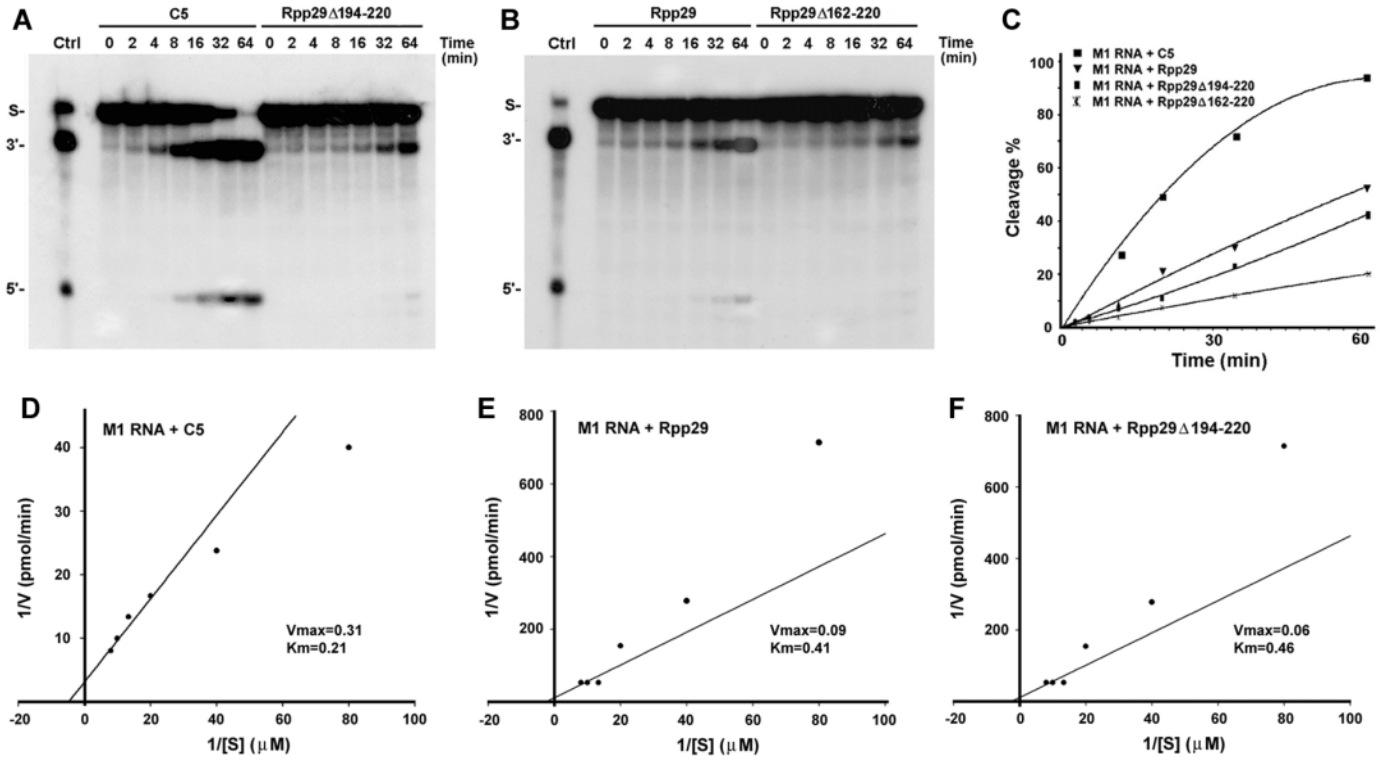

Figure 2. Kinetic analysis of substrate cleavage by M1 RNA reconstituted by various protein cofactors. (**A**) Time course of cleavage of 0.07 μM of p*SupS1* by 0.025 μM of M1 RNA reconstituted with 0.25 μM of Rpp29Δ194-220 or 0.25 μM of C5 protein. Reaction volumes were 150 μl and incubation was at 37°C. Small aliquots of 10 μl each were withdrawn at the following time points: 0, 2, 4, 8, 16, 32 and 64 min and mixed immediately with 10 μl of Urea dye. An aliquot withdrawn immediately after addition of substrate to the processing reactions is considered zero time point. Cleavage products, tRNA (3′) and 5′ leader sequence (5′), were resolved in 8% polyacrylamide/7 M urea gel. (**B**) Time course of cleavage of p*SupS1* as in (A) but 0.25 μM of recombinant Rpp29 and Rpp29Δ162-220 were used in the reconstitution assays with M1 RNA. (**C**) Graphic representation of the time course of substrate cleavage seen in (A and B). Substrate cleavage may vary by <10%. (**D**–**F**) Lineweaver–Burk plots obtained for substrate cleavage by M1 RNA reconstituted with C5 protein, Rpp29 or Rpp29Δ194-220 as indicated. Calculated V_{max} and K_m values are shown (Materials and Methods). Cleavage reactions were performed as described in (A) but increasing concentrations of unlabeled p*SupS1* (0.025–0.125 μM) were tested.

Table 1. Kinetic parameters of p*SupS1* cleavage by M1 RNA reconstituted by various protein cofactors

	M1 RNA C5	Rpp29	Rpp29Δ194-220	Rpp29Δ162-220	Rpp29Δ1-124
V_{max} (pmol min^{-1})	0.3	0.1	0.06	0.001	0.08
K_m (μM)	0.2	0.41	0.46	—	0.22
k_{cat} (min^{-1})	18	5.2	3.4	—	0.41
k_{cat}/K_m (min^{-1} μM^{-1})	90	12.7	7.4	—	1.86

Assay conditions were as described in Materials and Methods. Dialyzed Rpp29 produces a K_m value that is different from that reported for denatured Rpp29 used in reconstitution assays with M1 RNA (17). The data represent at least three independent determinations and the kinetic values exhibited a variation of <10%.

concentrations of the M1 RNA and protein cofactor were 0.01 and 0.1 μM, respectively (Figure 3A). The activity of M1 RNA–Rpp29 was inhibited at substrate concentrations of 0.5 and 1 μM (Figure 3A, lanes 9–15 and Figure 3C). In contrast, the activity of M1 RNA–C5 was not noticeably affected by this range of concentrations of p*SupS1* (Figure 3B, lanes 7–17 and Figure 3D).

The observations described above reveal a difference between Rpp29 and the C5 protein, where high concentrations of p*SupS1* impede the activity of M1 RNA reconstituted by the former protein. We assumed that this difference may be related to substrate binding properties of these two protein cofactors (see below).

Substrate binding properties of wild-type and mutant Rpp29 proteins

It has been reported that type A and B of bacterial RNase P proteins bind to precursor tRNA (28,29). We thus examined if Rpp29 can bind to precursor tRNA *in vitro*. Thus, gel shift analysis in 2× TNET buffer was performed with labeled p*SupS1* and increasing concentrations of dialyzed (Figures 4A) or denatured (Figure 4B) Rpp29 proteins. A retarded complex (C) was seen in the presence of Rpp29 and its formation responded in a dose dependent manner to Rpp29 (Figure 4A and B). Dialyzed and denatured Rpp29 proteins exhibited relatively high affinity in binding to

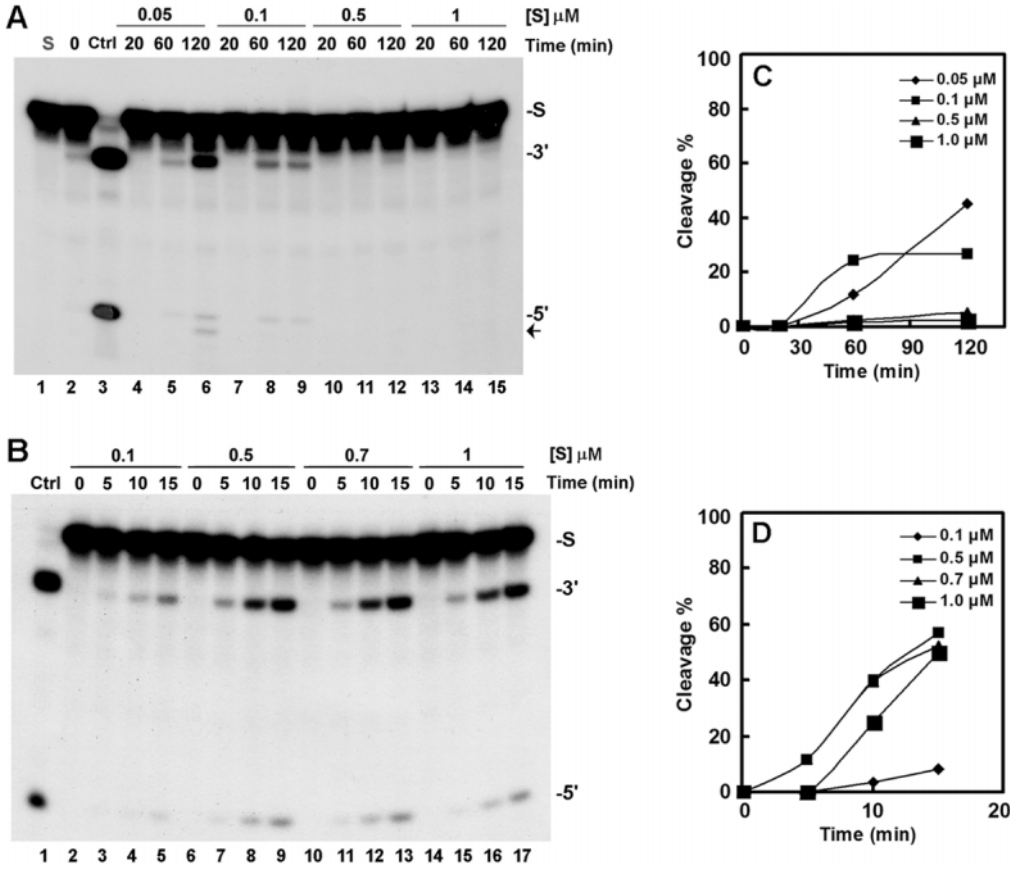

Figure 3. High substrate concentrations impede the activity of M1 RNA–Rpp29. (**A**) M1 RNA (0.01 μM) reconstituted with Rpp29 (0.1 μM) was tested for processing of p*SupS1* at concentrations ranging from 0.05 to 1 μM (Materials and Methods). Substrate (0.07 pmol) was ^{32}P-labeled p*SupS1* and the remaining was gel-purified, cold p*SupS1* RNA transcripts. Cleavage reactions (100 μl volume) proceeded at 37°C and small aliquots were withdrawn at the indicated time points (in minutes). Samples were resolved in denaturing 8% polyacrylamide gels. As controls, M1 RNA alone was tested in 1× RP buffer containing 10 and 80 mM $MgCl_2$ (lanes 2 and 3, respectively). The positions of p*SupS1* (S), tRNA and 5′ leader sequence are indicated. The shorter 5′ leader sequence indicated by an arrow resulted from incorrect substrate cleavage. (**B**) Cleavage reactions similar to those shown in (A) were performed with 0.01 μM of M1 RNA and 0.1 μM of recombinant C5 protein. Substrate concentrations and time points in minutes are indicated. (**C**) Graphic representation of the time course of substrate cleavage seen in (A). Percentage of cleavage of substrate at various concentrations is expressed as a function of time. Substrate cleavage may vary by <10%. (**D**) Graphic representation of the time course of substrate cleavages seen in (B). Percentage of cleavage of substrate at various concentrations is expressed as a function of time. Substrate cleavage may vary by <10%.

p*SupS1* with apparent K_d values of ∼1.2 and 2 μM, respectively (Figure 4A and B). In contrast, C5 protein did not form a stable complex with p*SupS1* (Figure 4A and B, lane 9). In effect, the C5 protein did not exhibit non-specific interaction with RNA (38) under the binding conditions tested. Competition assays with unlabeled p*SupS1* abolished complex formation by Rpp29 (data not shown).

Rpp29Δ194-220 weakly bound to the substrate, when compared with wild-type Rpp29 (Figure 4C, lanes 6–9 versus 2–5), while no complex was formed in the presence of Rpp29Δ162-220 (Figure 4C, lanes 10–13).

Binding of Rpp29 to precursor tRNA was further corroborated by northwestern blot analysis using labeled p*SupS1* in a hybridization buffer that contained 200 mM NaCl (Figure 4E; Materials and Methods). Rpp29 bound to the substrate (Figure 4E, lane 3), while Rpp20 and Rpp30 failed to do so (Figure 4E, lanes 2 and 6), even though equal amounts of proteins were analyzed (Figure 4D). However, in contrast to the results of the gel shift assays, Rpp29Δ194-220 and Rpp29Δ162-220 also produced binding signals (Figure 4E, lanes 4 and 5, respectively). Therefore, we first blocked the membrane with cold M1 RNA and then rehybridized the washed membrane with labeled p*SupS1* (Figure 4F). Rpp29Δ162-220 showed very faint, if any, binding signal (Figure 4F, lane 5), a result that was consistent with the gel shift assays, in which this truncated protein failed to interact with the substrate in solution (Figure 4C, lanes 10–13). Since this analysis is qualitative, no difference was observed in the binding signals produced by Rpp29 versus Rpp29Δ194-220 (Figure 4F, lane 3 versus 4).

The above findings reveal that Rpp29 interacts with precursor tRNA in the absence or presence of M1 RNA. Of note, high concentrations of Mg^{2+} ions (>10 mM) reduce the capability of Rpp29 to bind to precursor tRNA (E. Sharin and N. Jarrous, data not shown).

Rpp29 recognizes the 5′ leader sequence of precursor tRNA

The ability of Rpp29 to bind to p*SupS1* or its mature tRNA that lacks 5′ leader sequence was analyzed simultaneously by gel shift assays under conditions of 1× MK buffer (Figure 5;

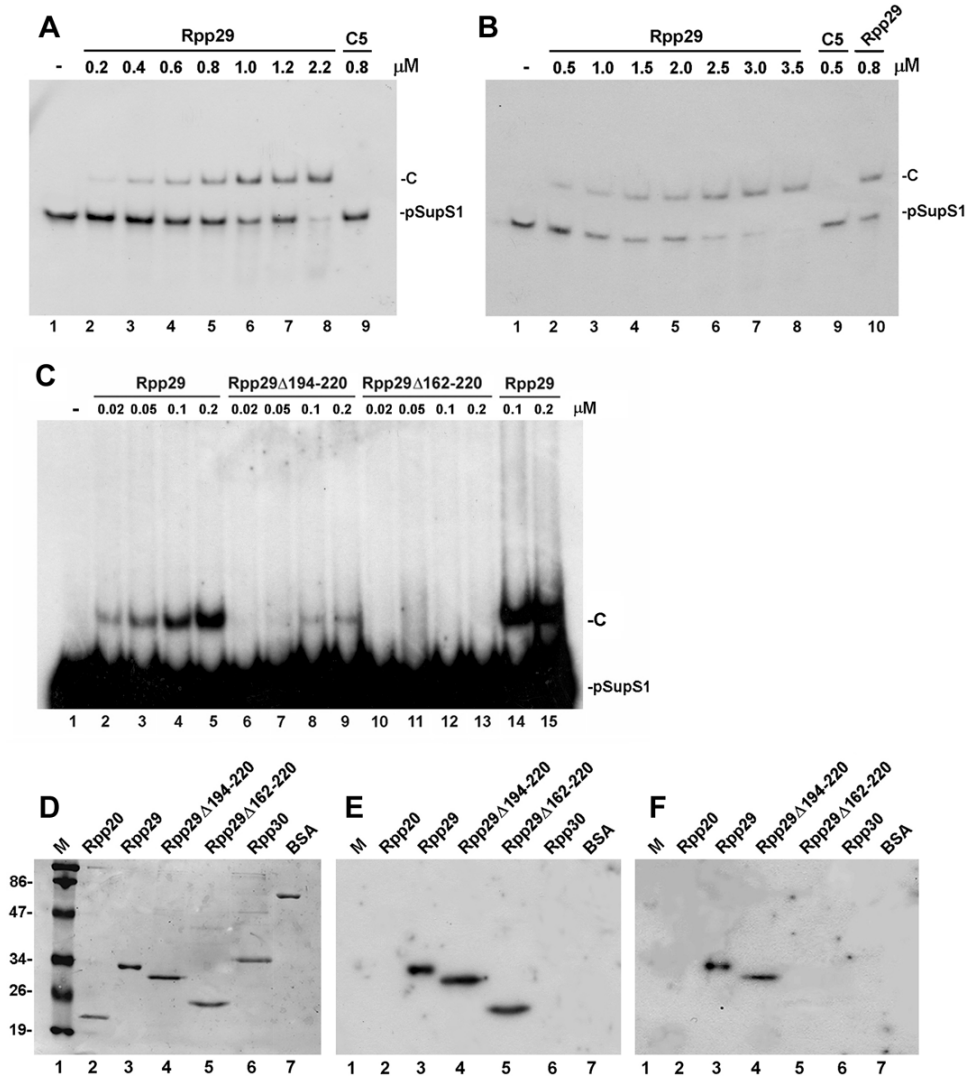

Figure 4. Binding of wild-type and mutant Rpp29 proteins to precursor tRNA. (**A**) Gel shift analysis of binding of Rpp29 to precursor tRNA. Increasing concentrations (0.2–2.2 μM) of dialyzed Rpp29 (lanes 2–8) or 0.8 μM of C5 protein were incubated with 2.66 nM of p*SupS1* in 100 μl of 2× TNET buffer for 30 min on ice (Materials and Methods). Samples were resolved in native 4% polyacrylamide gel. The gel was dried and bands were visualized by autoradiography. Position of complex (C) is shown. (**B**) Gel shift assays using increasing concentrations of denatured Rpp29 (Materials and Methods). For comparison, dialyzed Rpp29 (0.8 μM; lane 10) and C5 protein (0.5 μM; lane 9) were tested under the same binding conditions. (**C**) Electrophoretic mobility shift analysis of binding of wild-type and mutant Rpp29 polypeptides to p*SupS1*. The indicated concentrations (in μM) of denatured Rpp29 (lanes 2–5), Rpp29Δ194-220 (lanes 6–9), Rpp29Δ162-220 (lanes 10–13) or dialyzed Rpp29 (lanes 14 and 15) were incubated with 2.66 nM of labeled p*SupS1* in 2× TNET buffer (Materials and Methods). The 30 μl samples were resolved in native 4% polyacrylamide gel (40:0.5 acrylamide/bis) that was dried and bands were visualized by autoradiography. (**D**–**F**) Northwestern blot analysis of binding of wild-type and mutant Rpp29 polypeptides to p*SupS1*. The indicated proteins (20 pmol each) were separated in 12% SDS–PAGE and then transferred onto nitrocellulose membrane that was subsequently stained with Ponceau red (D) (Materials and Methods). The membrane was hybridized directly with ^{32}P-labeled p*SupS1* (1×10^6 c.p.m.) (E) or first pre-hybridized with unlabeled M1 RNA (5 μg) (F) and then hybridized with labeled p*SupS1* (1×10^6 c.p.m.). Bands were visualized by autoradiography. Protein size markers in kDa are shown.

Materials and Methods). Rpp29 and p*SupS1* formed two major complexes, C1 and C2 (Figure 5A, lane 4) while a larger complex, C3, was seen in longer exposures of this gel (data not shown). In the presence of mature tRNA, no C2 complex was seen and formation of the C1 complex was reduced (Figure 5A, lane 10 versus lane 4). The subunit Rpp21, which has been shown to interact with precursor tRNA (14), bound both to precursor and mature tRNA species (Figure 5A, lane 2 versus lane 8). Neither the subunit Rpp20 nor Rpp40 formed any complex with p*SupS1* (Figure 5A, lanes 5 and 6) or its mature tRNA form (Figure 5A, lanes 11 and 12). Similar complexes have been obtained when *E.coli* precursor tRNA^{Tyr} and its mature tRNA form were examined (data not shown).

The interaction of Rpp29 with p*SupS1* was further investigated by oligonucleotide binding interference assays. Short deoxyoligonucleotides complementary to the 5′ leader sequence (5′O), the D stem–loop (DO), the anticodon stem–loop (ACO) and the T stem–loop and acceptor stem (TO) (Figure 5C) were allowed to anneal to p*SupS1* (Figure 5B, lanes 2–6; and data not shown) before addition of Rpp29 to the binding reaction (Figure 5B, lanes 8–12). The 5′O and DO oligonucleotides inhibited the formation of the complex between Rpp29 and the substrate (Figure 5B,

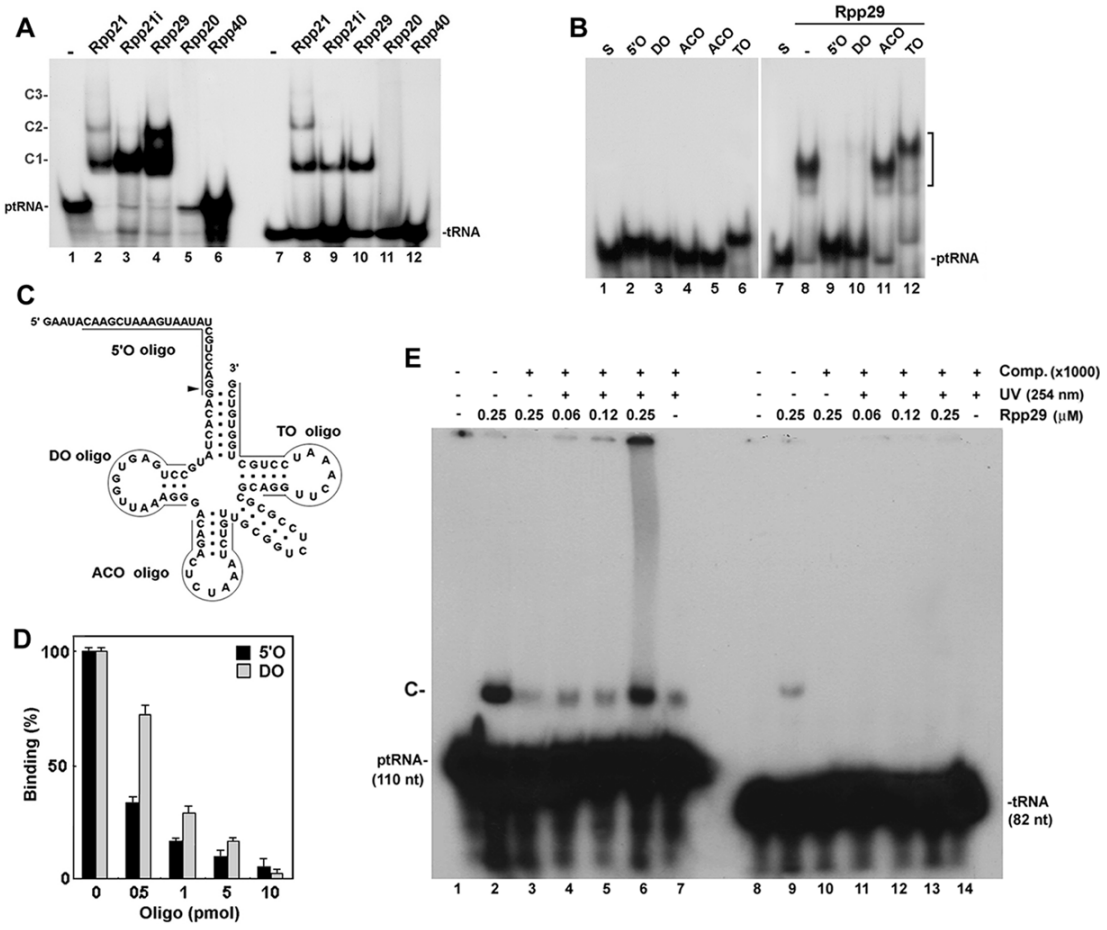

Figure 5. Binding of Rpp29 to precursor and mature tRNA. (**A**) Labeled p*SupS1* or its tRNA that lacks the 5′ leader sequence were incubated with recombinant Rpp21 (lanes 2 and 8), Rpp21i (lanes 3 and 9), Rpp29 (lanes 4 and 10), Rpp20 (lanes 5 and 11) or Rpp40 (lanes 6 and 12) in 1× MK buffer (Materials and Methods). RNA–protein complexes, C1, C2 and C3 were resolved in native 5% polyacrylamide gel. The use of precursor tRNA (lane 1) or mature tRNA (lane 7) made no difference in the electrophoretic mobility of the complexes. (**B**) Labeled p*SupS1* substrates (0.03 pmol; lanes 1 and 7) were annealed with 100 pmol of 5′O (lanes 2 and 9), DO (lanes 3 and 10), ACO (lanes 4 and 11) or TO (lanes 6 and 12) oligonucleotide in a total volume of 40 μl containing 1× BB buffer (Materials and Methods). In lane 5, 200 pmol of ACO oligonucleotide were included. Denatured Rpp29 (3 μM) (lanes 8–12) was added and complex formation was analyzed by gel shift assays as described in (A). The two parts of this panel were derived from the same film exposure. (**C**) Schematic representation of p*SupS1* with the 5′O, DO, ACO and TO oligonucleotides used in this study. Cleavage site of M1 RNA–Rpp29 is indicated by an arrow. (**D**) Percentage of binding interference as a function of the amount of 5′O and DO oligonucleotides. Increasing amounts of 5′O or DO oligonucleotides (0, 0.5, 1, 5 and 10 pmol) were incubated with p*SupS1* for annealing before gel shift assays were performed in the presence of denatured Rpp29 as described in (C). (**E**) ^{32}P-labeled p*SupS1* (lane 1) or mature tRNA form (lane 8) (4.5 nM) was incubated with the indicated concentrations of recombinant Rpp29 (lanes 2–6 and lanes 9–13, respectively) in 1 × TNET buffer containing 2 mM $MgCl_2$. Samples were subjected to UV-crosslinking (at UV light of 254 nm) for 90 s (lanes 4–7 and lanes 11–14) or were left untreated (lanes 1–3 and lanes 8–10). Except for lanes 2 and 9, excess amount (4.5 μM) of cold p*SupS1* (lanes 3–7) or mature tRNA (lanes 10–14) was added as specific competitors. After 10 min at 37°C, all samples were resolved in native 4% polyacrylamide gel and bands were visualized by radiography. An intramolecular crosslink of p*SupS1*, which migrates slightly faster than the Rpp29–p*SupS1* complex (C) is seen in lane 7. Higher concentrations (0.5 and 1 μM) of Rpp29 did not enhance the crosslinking signal under the same experimental conditions (data not shown).

lane 8 versus lanes 9 and 10), while the ACO and TO oligonucleotides had no effect (Figure 5B, lanes 11 and 12). Dose response experiments revealed that binding of Rpp29 to the substrate was more sensitive to the inhibitory effect of the 5′O oligonucleotide than that of the DO oligonucleotide (Figure 5D). Thus, Rpp29 recognizes the 5′ leader sequence and may contact the DO of the precursor tRNA.

The above conclusion is supported by UV-crosslinking analysis in which we showed that recombinant Rpp29 protein could be crosslinked efficiently to p*SupS1* (Figure 5E, lanes 1–7) but not to its mature tRNA form (Figure 5E, lanes 8–14), suggesting that the substrate rather than the product is primarily recognized by Rpp29.

Rpp29 directly binds to M1 RNA

The impaired activity of M1 RNA observed in the presence of the truncated mutants of Rpp29, when compared with the wild-type protein, could also be due to lack of interaction of these mutants with M1 RNA. To examine this possibility, northwestern blot analysis was performed using full length, ^{32}P-labeled M1 RNA as a probe (Figure 6A). Rpp29 produced a binding signal with M1 RNA (Figure 6A, lane 4), while the subunits Rpp20, Rpp21 and Rpp30 failed to interact with this RNA (Figure 6A, lanes 1–3 and 7) or activate it (data not shown). Rpp29Δ194-220 and Rpp29Δ162-220 also produced binding signals with M1 RNA (Figure 6A, lanes 5 and 6). Similar results were obtained when a similar analysis was

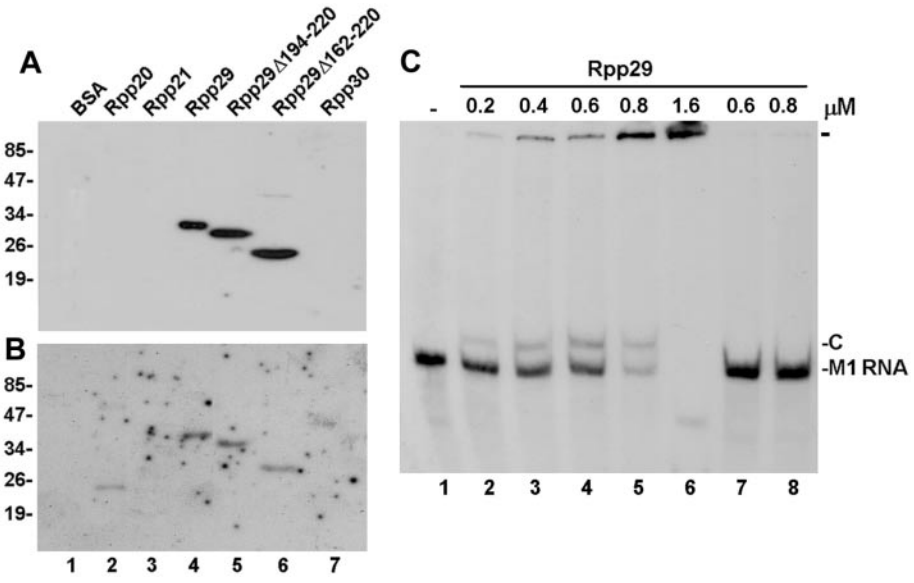

Figure 6. Binding of Rpp29 to M1 RNA. (**A**) Northwestern blot analysis of binding of Rpp29 to M1 RNA. The indicated proteins (20 pmol each) were separated in 12% SDS–PAGE and then transferred onto nitrocellulose membrane that was hybridized with 1×10^6 c.p.m. of ^{32}P-labeled M1 RNA (Materials and Methods). Bands were visualized by autoradiography. Recombinant proteins and protein size markers were visualized by staining of the membrane with Ponceau red (data not shown). (**B**) Northwestern blot analysis using a ^{32}P-labeled RNase MRP RNA (265 nt) as probe. (**C**) Gel shift analysis of binding of Rpp29 to M1 RNA. Increasing concentrations of dialyzed Rpp29 (lanes 2–8) were incubated with 2.6 nM of internally ^{32}P-labeled M1 RNA in 2× TNET buffer (Materials and Methods). The 100 μl samples were resolved in native 4% polyacrylamide gel and the radioactive bands were visualized by autoradiography. Position of the M1 RNA–Rpp29 complex (C) is shown. Complexes of M1 RNA–Rpp29 remained in the gel wells when high concentrations of Rpp29 were used (lanes 5 and 6). Lanes 7 and 8 show inhibition of complex formation by unlabeled M1 RNA used as a specific competitor.

performed with a membrane that was blocked with an excess amount of unlabeled p*SupS1* before addition of labeled M1 RNA (data not shown). Notably, Rpp21 bound to precursor tRNA (Figures 5A) but not to M1 RNA (Figure 6A), suggesting that the putative tRNA-binding site in Rpp21 was not used for non-specific interaction with M1 RNA. Moreover, when a ^{32}P-labeled RNase MRP RNA was tested as control, both Rpp29 and Rpp20 produced binding signals (Figure 6B). Thus, this hybridization method allows the identification of proteins that bind to different RNAs but cannot provide quantitative analysis for distinct or similar proteins that bind to the same RNA.

The ability of Rpp29 to interact with M1 RNA was examined by gel shift assays. A specific complex was formed between M1 RNA and Rpp29 (Figure 6C, lanes 2–6). Rpp29 at high concentrations formed large complexes with M1 RNA that remained in the gel wells (Figure 6C, lanes 5 and 6). Of note, 50% binding of Rpp29 to M1 RNA was seen at $\geq$0.8 μM (Figure 6C, lane 5), suggesting that Rpp29 has a relatively high binding affinity to M1 RNA. Nonetheless, this binding affinity is several magnitude lower than that obtained for binding of the C5 protein to M1 RNA (K_d = 0.4 nM) (33,38).

The results described above, combined with the enzyme kinetic data, reveal that Rpp29 exhibits dual RNA binding capabilities, one for binding to M1 RNA and the other for interacting with the tRNA substrate.

The C-terminal domain of Rpp29 can activate M1 RNA

To have direct evidence that the C-terminal domain of Rpp29 is responsible for activation of M1 RNA, we constructed a truncation mutant, Rpp29Δ1-124, which lacks the first 124 amino acids of Rpp29 (Figure 7A; Materials and Methods), and tested the resulted recombinant protein in reconstitution assays with M1 RNA. Rpp29Δ1-124 was able to activate M1 RNA in processing of p*SupS1* (Figure 7C), with optimal activity measured at a molar ratio of 1:40 (Figure 7C). The 2D thin layer chromatography revealed pGp as the 5′ end group of tRNA products generated in cleavage reactions of p*SupS1* by M1 RNA reconstituted with Rpp29Δ1-124 (Figure 7B). Time course analysis of substrate cleavage by M1 RNA reconstituted by Rpp29Δ1-124 at molar ratios of 1:20 or 1:40 showed that this protein was less effective by ~7-fold than wild-type Rpp29 in activation of M1 RNA (Figure 7D), a conclusion that is also supported by comparing the catalytic efficiencies, k_{cat}/K_m, of these two proteins (Table 1). Rpp29Δ1-124 retained its capability to bind to precursor tRNA as determined by gel shift assay (Figure 7F, lanes 2–4).

Conserved amino acid residues in the C-terminal domain of Rpp29 are critical for M1 RNA activation

Structure comparative analyses of archaeal and eukaryal Rpp29 proteins reveal that the C-terminal domain of human Rpp29 may acquire an Sm-like fold (22,24), as also predicted in Figure 7A. We examined two structural motifs in this potential Sm-like fold: the conserved KH motif (Lys162 and His163) proposed to contact the RNase P RNA and the potential three-way salt bridge, wherein Lys179 is highly conserved (Figure 7A, asterisks) (22,24). Thus, we substituted Lys162 and His163 with two asparagine residues in Rpp29KH and replaced Lys179 with asparagine in another mutant, Rpp29K179N (Materials and Methods). Time course analysis of substrate cleavage revealed that Rpp29KH served as a weak cofactor in activation of M1 RNA (Figure 7E). In contrast, Rpp29K179N stimulated M1 RNA activity more efficiently

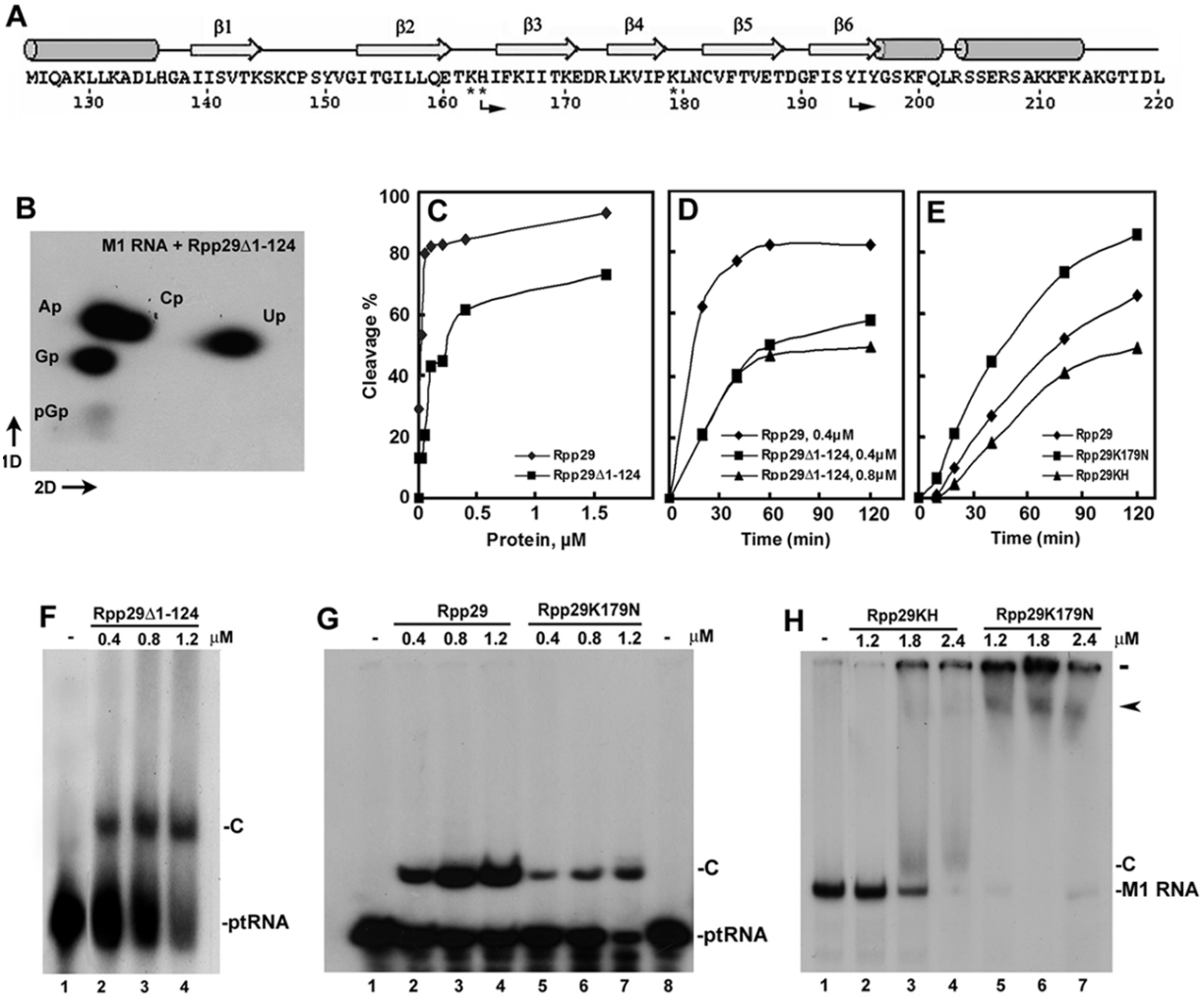

Figure 7. The C-terminal domain of Rpp29 is responsible for activation of M1 RNA. (**A**) Secondary structure of the C-terminal domain of Rpp29 as predicted by the PSIPRED Protein Structure Prediction software (39). α-helices are shown as cylinders, β-strands as arrows and turns as lines. An array of six β-strands that may form an Sm-like fold spans amino acid residues at positions 125–220 of Rpp29. Sm-like folds of six anti-parallel β-strands exist in archaeal Rpp29 counterparts (22,24). Bold arrows indicate the starts of the Rpp29Δ162-220 and Rpp29Δ194-220 mutants. Asterisks point to amino acids that were substituted in Rpp29KH and Rpp29K179N. (**B**) The 2D thin layer chromatography of tRNA products of cleavage reactions of p*SupS1* by M1 RNA–Rpp29Δ1-124. Gp, Ap, Cp, Up and pGp are shown. Arrows point to the first and second dimension of the chromatography. (**C**) Increasing concentrations of recombinant Rpp29 and Rpp29Δ1-124 polypeptides were tested for activation of 0.02 μM of M1 RNA. Cleavage of 0.07 μM of p*SupS1* was for 120 min at 37°C. Substrate and cleavage products were resolved in 8% polyacrylamide/7 M urea gel, bands were quantified and plotted as percentage of substrate cleavage per protein concentration. Substrate cleavage may vary by <10%. (**D**) Time course of p*SupS1* substrate cleavage by M1 RNA (0.02 μM) reconstituted with wild-type Rpp29 at a molar ratio of 1:20 or with Rpp29Δ1-124 at molar ratios of 1:20 and 1:40. Substrate and cleavage products were resolved in 8% polyacrylamide/7 M urea gel, bands were quantified and plotted as percentage of cleavage per time (in minutes). Substrate cleavage may vary by <10%. (**E**) Time course of substrate cleavage by M1 RNA (0.02 μM) reconstituted with wild-type Rpp29, Rpp29KH or Rpp29K179N at molar ratios of 1:20. Substrate cleavage analysis was as in (D). (**F**) Gel shift analysis that shows binding of p*SupS1* by the indicated concentrations of Rpp29Δ1-124. Binding conditions and analysis of complexes were as described in Figure 4A. (**G**) Gel shift analysis of p*SupS1* binding by wild-type Rpp29 (lanes 2–4) and Rpp29K179N (lanes 5–7) at the indicated concentrations. Binding conditions and analysis of complexes were as described in Figure 4A. (**H**) Binding of M1 RNA by the indicated concentrations of Rpp29KH (lanes 2–4) or Rpp29K179N (lanes 5–7). Binding conditions and analysis of complexes (C) were as described in Figure 4B. Arrow points to large complexes of Rpp29K179N formed with M1 RNA.

than Rpp29 (Figure 7E). Rpp29K179N bound to the substrate less efficiently than Rpp29 (Figure 7G, lanes 2–4 versus lanes 5–7) but we found no change in substrate binding capability of Rpp29KH (data not shown). Comparison of the M1 RNA binding capabilities of these two mutants revealed that Rpp29KH did not bind to M1 RNA at 1.2 μM protein concentration (Figure 7H, lane 2), while Rpp29K179N shifted the M1 RNA to large complexes that entered the gel (Figure 7H, lanes 5–7; arrow).

The above findings demonstrate that substitution of the KH motif in Rpp29 affects its interaction with M1 RNA, while replacing lysine with asparagine at position 179 reduces the binding affinity of the mutant protein to precursor tRNA and improves the catalytic efficiency of M1 RNA.

DISCUSSION

Properties of the M1 RNA–Rpp29 chimeric ribonucleoprotein

We have shown that M1 RNA and Rpp29 form a catalytic ribonucleoprotein that exhibits high binding affinity to tRNA

substrates and facilitates multiple turnover cleavage reactions. Nonetheless, M1 RNA–Rpp29 is catalytically less effective than the M1 RNA–C5 complex.

Rpp29 has a role in substrate recognition that is mediated by its C-terminal domain. Thus, Rpp29 may augment the catalytic efficiency of M1 RNA by facilitating direct interaction with precursor tRNA.

The heterologous reconstitution of M1 RNA activity with Rpp29 as described in this study has several new enzymological and biological insights. First, heterologous reconstitution systems developed for bacterial RNase P ribonucleoproteins (RNPs) have produced novel findings related to the importance of the structure rather than the primary amino acid sequences of bacterial protein subunits in holoenzyme function (24,29,35). The ability of Rpp29 to activate M1 RNA further emphasizes the dependence of this RNA catalyst on the structure of its interacting protein. Second, in contrast to the homologous reconstitution system of human mini-RNase P that involves at least three components, e.g. Rpp21, Rpp29 and H1 RNA (17), which makes it difficult to elucidate the exact role and contribution of each subunit in substrate recognition and catalysis, the simple nature of the heterologous reconstitution system of M1 RNA and Rpp29 allows the examination of the role of this protein cofactor in substrate binding and catalysis. Third, M1 RNA is functional in mammalian cells as a targeting ribozyme in the presence of external guide sequences (40) and purified human RNase P protein preparations have been shown to activate M1 RNA *in vitro* (40), thus strengthening the biological relevance of our study on activation of M1 RNA by Rpp29.

A major difference between the C5 protein and Rpp29 in activation of M1 RNA is that the latter protein cofactor can facilitate multiple turnover reactions of substrate cleavage as long as substrate concentration is <0.5 μM (Figure 3), a value that is close to the calculated K_m value of M1 RNA–Rpp29 (Table 1). In contrast, M1 RNA–C5 remains active when substrate concentrations are high, well above the K_m value. Rpp29 itself has a relatively high binding affinity to precursor tRNA. Our gel shift assays reveal that the C5 protein does not bind to p*SupS1* under conditions that facilitate binding by Rpp29 (Figure 4). Lack of or weak interaction of the C5 protein alone with precursor tRNA may explain why high concentrations of substrate do not inhibit the activity of the holoenzyme. In contrast, C5 protein has been shown to exhibit a very high binding affinity ($K_d = 0.4$ nM) to its natural M1 RNA partner (33,38).

Protein folds and RNase P RNA-based catalysis

Rpp29 is conserved in Eucarya and Archaea (19,21) and is composed of two major domains (41). The most conserved part of Rpp29 corresponds to its C-terminus, while the N-terminal part of Rpp29, which harbors nuclear/nucleolar localization domains (42), is preserved among eukaryotic homologs. The C-terminal domain of Rpp29 promotes direct interactions with precursor tRNA and M1 RNA. A truncation mutant of Rpp29, Rpp29Δ1-124, which has the C-terminal part that possesses an Sm-like fold, is sufficient for substrate binding and activation of M1 RNA. Such dual RNA-binding capabilities have also been proposed for the C5 protein (35). The role of Rpp29 and C5 protein in substrate recognition and catalysis is different from those reported for other protein cofactors of RNA catalysts, such as the *Saccharomyces cerevisiae* CBP2 and *Neurospora crassa* CYT-18, which facilitate the tertiary folding of the *S.cerevisiae* mitochondrial bI5 group I intron RNA (43) or the LtrA protein that stabilizes the catalytically active structure of *Lactococcus lactis* Ll.LtrB group II intron (44).

The 3D structures of human Rpp29 and C5 protein are not available. Nonetheless, the tertiary structures of the RNase P proteins from *B.subtilis*, *Staphylococcus aureus* and *Thermotoga maritima* have been resolved (34,45,46). These bacterial proteins share a homologous structure that bears several potential RNA-binding sites, e.g. a central cleft, a metal-binding loop and an RNR motif (29). The central cleft in the *B.subtilis* RNase P protein and the C5 protein probably mediates interaction with precursor tRNA (27–29). The predicted secondary structure (39) of the C-terminus of human Rpp29 reveals an array of six β-strands with α-helices at both sides typical of an Sm-like fold (Figure 7A) (22,24) that may interact with RNA (19,22–24,47,48). Of note, archaeal Sm proteins have been shown to bind to RNase P RNA (48). Based on our mutational analysis, the KH motif, which is located in the loop between the β2 and β3 strands in Rpp29 (Figure 7A) (22,24) may contact the M1 RNA. Based on structural studies, these two amino acid residues in Rpp29 have been proposed to be involved in RNase P RNA–protein interaction (22,24). In contrast, substitution of Lys179, which is found in the loop between the β4 and β5 strands of Rpp29 (Figure 7A) (24) affects substrate binding. Lys179 in human Rpp29 corresponds to Lys58 in the *A.fulgidus* Rpp29 that is part of a three-way salt bridge proposed to have a role in protein stability (24). Since substitution of Lys179 in Rpp29 alters the RNA binding properties of Rpp29, this conserved residue (19,22,24) may have a unique role in shaping or stabilizing the global structure of the protein (24). Work is in progress to examine the effect of substitution of Lys179 to amino acids other than asparagine (this polar residue can be part of salt bridges in proteins) on activation of M1 RNA and human mini-RNase P (E. Sharin and N. Jarrous, unpublished data). In addition, since Rpp29 is also a core component of RNase MRP, substitution of Lys179 may also affect RNase MRP function in rRNA processing (49,50).

The distinct structures of bacterial RNase P proteins and archaeal/eukaryal Rpp29 suggest that these ancient protein cofactors belong to unrelated protein families with analogous functions in RNase P RNA-based catalysis (41). Nonetheless, these proteins are structurally and genetically linked to ribosomal proteins and translation factors (17,22,34,45,46). Thus, archaeal Rpp29 proteins exhibit topological resemblance to the bacterial translational regulator Hfq (22,24) and *Haloarcula marismortui* ribosomal protein L21 (22), both of which possess Sm-like folds (22,24). The protein subunit of *B.subtilis* RNase P shares common structural features with ribosomal protein S5 and the ribosomal translocase EF-G (45). Translation of bacterial RNase P proteins and the ribosomal protein L34 overlaps in bacteria while Rpp29 coding genes are embedded in ribosomal protein operons in archaea (51). The genetic links and structural resemblance of these highly conserved basic proteins, probably derived from ancient RNA-binding peptides (52), suggest that they have emerged and evolved

during transition of the ribosome and RNase P from RNA to RNP enzymes.

ACKNOWLEDGEMENTS

We thank Sidney Altman (Yale University) for providing us with recombinant C5 protein and anti-C5 protein antibodies. Y.B.A., a postdoctoral fellow, is supported in part by the anonymous fund with Dr Nemeth, Friends of the Hebrew University, UK. This research is supported by the United States-Israel Binational Science Foundation (grant no. 2001-017), the Israel Science Foundation (grant no. 549/01) and the Abisch-Frenkel Foundation (Switzerland) to N.J. Funding to pay the Open Access publication charges for this article was provided by United States-Israel Binational Science Foundation.

Conflict of interest statement. None declared.

REFERENCES

1. Jarrous,N. and Altman,S. (2001) Human ribonuclease P. *Methods Enzymol*., **342**, 93–100.
2. Dragon,F., Gallagher,J.E., Compagnone-Post,P.A., Mitchell,B.M., Porwancher,K.A., Wehner,K.A., Wormsley,S., Settlage,R.E., Shabanowitz,J., Osheim,Y. *et al.* (2002) A large nucleolar U3 ribonucleoprotein required for 18S ribosomal RNA biogenesis. *Nature*, **417**, 967–970.
3. Zhou,Z., Licklider,L.J., Gygi,S.P. and Reed,R. (2002) Comprehensive proteomic analysis of the human spliceosome. *Nature*, **419**, 182–185.
4. Fatica,A. and Tollervey,D. (2003) Insights into the structure and function of a guide RNP. *Nature Struct. Biol*., **10**, 237–239.
5. Eddy,S.R. (2001) Non-coding RNA genes and the modern RNA world. *Nature Rev. Genet*., **2**, 919–929.
6. Storz,G. (2002) An expanding universe of noncoding RNAs. *Science*, **296**, 1260–1263.
7. Villa,T., Pleiss,J.A. and Guthrie,C. (2002) Spliceosomal snRNAs: Mg(2+)-dependent chemistry at the catalytic core? *Cell*, **109**, 149–152.
8. Altman,S. (2000) The road to RNase P. *Nature Struct. Biol*., **7**, 827–828.
9. Kirsebom,L.A. (2001) *Escherichia coli* ribonuclease P. *Methods Enzymol*., **342**, 77–92.
10. Schön,A. (1999) Ribonuclease P: the diversity of a ubiquitous RNA processing enzyme. *FEMS Microbiol. Rev*., **23**, 391–406.
11. Lygerou,Z., Pluk,H., van Venrooij,W.J. and Seraphin,B. (1996) hPop1: an autoantigenic protein subunit shared by the human RNase P and RNase MRP ribonucleoproteins. *EMBO J*., **15**, 5936–5948.
12. Eder,P.S., Kekuda,R., Stolc,V. and Altman,S. (1997) Characterization of two scleroderma autoimmune antigens that copurify with human ribonuclease P. *Proc. Natl Acad. Sci. USA*, **94**, 1101–1106.
13. Jarrous,N., Eder,P.S., Guerrier-Takada,C., Hoog,C. and Altman,S. (1998) Autoantigenic properties of some protein subunits of catalytically active complexes of human ribonuclease P. *RNA*, **4**, 407–417.
14. Jarrous,N., Reiner,R., Wesolowski,D., Mann,H., Guerrier-Takada,C. and Altman,S. (2001) Function and subnuclear distribution of Rpp21, a protein subunit of the human ribonucleoprotein ribonuclease P. *RNA*, **7**, 1153–1164.
15. van Eenennaam,H., Lugtenberg,D., Vogelzangs,J.H., van Venrooij,W.J. and Pruijn,G.J. (2001) hPop5, a protein subunit of the human RNase MRP and RNase P endoribonucleases. *J. Biol. Chem*., **276**, 31635–31641.
16. Guerrier-Takada,C., Eder,P.S., Gopalan,V. and Altman,S. (2002) Purification and characterization of Rpp25, an RNA-binding protein subunit of human ribonuclease P. *RNA*, **8**, 290–295.
17. Mann,H., Ben-Asouli,Y., Schein,A., Moussa,S. and Jarrous,N. (2003) Eukaryotic RNase P: role of RNA and protein subunits of a primordial catalytic ribonucleoprotein in RNA-based catalysis. *Mol. Cell*, **12**, 925–935.
18. Kouzuma,Y., Mizoguchi,M., Takagi,H., Fukuhara,H., Tsukamoto,M., Numata,T. and Kimura,M. (2003) Reconstitution of archaeal ribonuclease P from RNA and four protein components. *Biochem. Biophys. Res. Commun*., **306**, 666–673.
19. Boomershine,W.P., McElroy,C.A., Tsai,H.Y., Wilson,R.C., Gopalan,V. and Foster,M.P. (2003) Structure of Mth11/Mth Rpp29, an essential protein subunit of archaeal and eukaryotic RNase P. *Proc. Natl Acad. Sci. USA*, **100**, 15398–15403.
20. Houser-Scott,F., Xiao,S., Millikin,C.E., Zengel,J.M., Lindahl,L. and Engelke,D.R. (2002) Interactions among the protein and RNA subunits of *Saccharomyces cerevisiae* nuclear RNase P. *Proc. Natl Acad. Sci. USA*, **99**, 2684–2689.
21. Hall,T.A. and Brown,J.W. (2002) Archaeal RNase P has multiple protein subunits homologous to eukaryotic nuclear RNase P proteins. *RNA*, **8**, 296–306.
22. Numata,T., Ishimatsu,I., Kakuta,Y., Tanaka,I. and Kimura,M. (2004) Crystal structure of archaeal ribonuclease P protein Ph1771p from *Pyrococcus horikoshii* OT3: an archaeal homolog of eukaryotic ribonuclease P protein Rpp29. *RNA*, **10**, 1423–1432.
23. Sidote,D.J. and Hoffman,D.W. (2003) NMR structure of an archaeal homologue of ribonuclease P protein Rpp29. *Biochemistry*, **42**, 13541–13550.
24. Sidote,D.J., Heideker,J. and Hoffman,D.W. (2004) Crystal structure of archaeal ribonuclease P protein aRpp29 from *Archaeoglobus fulgidus*. *Biochemistry*, **43**, 14128–14138.
25. Guerrier-Takada,C., Gardiner,K., Marsh,T., Pace,N. and Altman,S. (1983) The RNA moiety of ribonuclease P is the catalytic subunit of the enzyme. *Cell*, **35**, 849–857.
26. Liu,F. and Altman,S. (1994) Differential evolution of substrates for an RNA enzyme in the presence and absence of its protein cofactor. *Cell*, **77**, 1093–1100.
27. Niranjanakumari,S., Stams,T., Crary,S.M., Christianson,D.W. and Fierke,C.A. (1998) Protein component of the ribozyme ribonuclease P alters substrate recognition by directly contacting precursor tRNA. *Proc. Natl Acad. Sci. USA*, **95**, 15212–15217.
28. Tsai,H.Y., Masquida,B., Biswas,R., Westhof,E. and Gopalan,V. (2003) Molecular modeling of the three-dimensional structure of the bacterial RNase P holoenzyme. *J. Mol. Biol*., **325**, 661–675.
29. Hsieh,J., Andrews,A.J. and Fierke,C.A. (2004) Roles of protein subunits in RNA–protein complexes: lessons from ribonuclease P. *Biopolymers*, **73**, 79–89.
30. Reich,C., Olsen,G.J., Pace,B. and Pace,N.R. (1988) Role of the protein moiety of ribonuclease P, a ribonucleoprotein enzyme. *Science*, **239**, 178–181.
31. Crary,S.M., Niranjanakumari,S. and Fierke,C.A. (1998) The protein component of *Bacillus subtilis* ribonuclease P increases catalytic efficiency by enhancing interactions with the 5′ leader sequence of pre-tRNA^{Asp}. *Biochemistry*, **37**, 9409–9416.
32. Pomeranz Krummel,D.A. and Altman,S. (1999) Multiple binding modes of substrate to the catalytic RNA subunit of RNase P from *Escherichia coli*. *RNA*, **5**, 1021–1033.
33. Talbot,S.J. and Altman,S. (1994) Kinetic and thermodynamic analysis of RNA–protein interactions in the RNase P holoenzyme from *Escherichia coli*. *Biochemistry*, **33**, 1406–1411.
34. Kazantsev,A.V., Krivenko,A.A., Harrington,D.J., Carter,R.J., Holbrook,S.R., Adams,P.D. and Pace,N.R. (2003) High-resolution structure of RNase P protein from *Thermotoga maritima*. *Proc. Natl Acad. Sci. USA*, **100**, 7497–7502.
35. Gopalan,V., Vioque,A. and Altman,S. (2002) RNase P: variations and uses. *J. Biol. Chem*., **277**, 6759–6762.
36. Kirsebom,L.A. and Vioque,A. (1995–96) RNase P from bacteria. Substrate recognition and function of the protein subunit. *Mol. Biol. Rep*, **22**, 99–109.
37. Pannucci,J.A., Haas,E.S., Hall,T.A., Harris,J.K. and Brown,J.W. (1999) RNase P RNAs from some Archaea are catalytically active. *Proc. Natl Acad. Sci. USA*, **96**, 7803–7808.
38. Vioque,A., Arnez,J. and Altman,S. (1988) Protein–RNA interactions in the RNase P holoenzyme from *Escherichia coli*. *J. Mol. Biol*., **202**, 835–848.
39. McGuffin,L.J., Bryson,K. and Jones,D.T. (2000) The PSIPRED protein structure prediction server. *Bioinformatics*, **16**, 404–405.
40. Liu,F. and Altman,S. (1995) Inhibition of viral gene expression by the catalytic RNA subunit of RNase P from *Escherichia coli*. *Genes Dev*., **9**, 471–480.
41. Chothia,C., Gough,J., Vogel,C. and Teichmann,S.A. (2003) Evolution of the protein repertoire. *Science*, **300**, 1701–1703.

42. Jarrous,N., Wolenski,J.S., Wesolowski,D., Lee,C. and Altman,S. (1999) Localization in the nucleolus and coiled bodies of protein subunits of the ribonucleoprotein ribonuclease P. *J. Cell Biol.*, **146**, 559–572.
43. Webb,A.E., Rose,M.A., Westhof,E. and Weeks,K.M. (2001) Protein-dependent transition states for ribonucleoprotein assembly. *J. Mol. Biol.*, **309**, 1087–1100.
44. Noah,J.W. and Lambowitz,A.M. (2003) Effects of maturase binding and Mg^{2+} concentration on group II intron RNA folding investigated by UV cross-linking. *Biochemistry*, **42**, 12466–12480.
45. Stams,T., Niranjanakumari,S., Fierke,C.A. and Christianson,D.W. (1998) Ribonuclease P protein structure: evolutionary origins in the translational apparatus. *Science*, **280**, 752–725.
46. Spitzfaden,C., Nicholson,N., Jones,J.J., Guth,S., Lehr,R., Prescott,C.D., Hegg,L.A. and Eggleston,D.S. (2000) The structure of ribonuclease P protein from *Staphylococcus aureus* reveals a unique binding site for single-stranded RNA. *J. Mol. Biol.*, **295**, 105–115.
47. Anantharaman,V. and Aravind,L. (2004) Novel conserved domains in proteins with predicted roles in eukaryotic cell-cycle regulation, decapping and RNA stability. *BMC Genomics*, **5**, 45.
48. Toro,I., Thore,S., Mayer,C., Basquin,J., Seraphin,B. and Suck,D. (2001) RNA binding in an Sm core domain: X-ray structure and functional analysis of an archaeal Sm protein complex. *EMBO J.*, **20**, 2293–2303.
49. Welting,T.J., van Venrooij,W.J. and Pruijn,G.J. (2004) Mutual interactions between subunits of the human RNase MRP ribonucleoprotein complex. *Nucleic Acids Res.*, **32**, 2138–2146.
50. Jarrous,N. (2002) Human ribonuclease P: subunits, function, and intranuclear localization. *RNA*, **8**, 1–7.
51. Hartmann,E. and Hartmann,R.K. (2003) The enigma of ribonuclease P evolution. *Trends Genet.*, **19**, 561–569.
52. Soding,J. and Lupas,A.N. (2003) More than the sum of their parts: on the evolution of proteins from peptides. *Bioessays*, **25**, 837–846.